

UT-04-27
hep-th/0410138
October 2004

On String Junctions in Supersymmetric Gauge Theories

Yosuke Imamura*

Department of Physics, University of Tokyo, Tokyo 113-0033, Japan

Abstract

We study junctions consisting of confining strings in $\mathcal{N} = 1$ supersymmetric large N gauge theories by means of the gauge/gravity correspondence. We realize these junctions as D-brane configurations in infrared geometries of the Klebanov-Strassler (KS) and the Maldacena-Núñez (MN) solutions. After discussing kinematics associated with the balance of tensions, we compute the energies of baryon vertices numerically. In the KS background, baryon vertices give negative contributions to the energies. The results for the MN background strongly suggest that the energies of baryon vertices exactly vanish, as in the case of supersymmetric (p, q) -string junctions. We find that brane configurations in the MN background have a property similar to the holomorphy of the M-theory realization of (p, q) -string junctions. With the help of this property, we analytically prove the vanishing of the energies of baryon vertices in the MN background.

*E-mail: imamura@hep-th.phys.s.u-tokyo.ac.jp

1 Introduction

The gauge/gravity correspondence[1, 2, 3] relates five-dimensional gravitational backgrounds to four-dimensional field theories on the boundaries of the five-dimensional spacetimes. The extra dimension r is related to the energy scales of the field theories through red-shift (warp) factors depending on r . The five-dimensional spacetimes are in general accompanied by compact internal spaces. The structures of these higher-dimensional spacetimes reflect non-perturbative properties of their dual field theories. Many gravity duals of various field theories have been constructed in the context of string theory as near horizon geometries of branes on which gauge theories are realized.

Various kinds of particles in boundary field theories are identified with a number of objects in string theory. These particles have been investigated with respect to the above-mentioned duality. Specifically, the spectra of glueballs[4, 5, 6, 7], mesons[8, 9, 10, 11, 12, 13, 14, 15] and (di-)baryons[16, 17, 18, 19, 20] and interactions among them[21, 22, 14] have been studied with a variety of methods. Bound states of massive adjoint or bifundamental particles are investigated in Refs. [23, 24, 25, 26, 27, 28, 29]. In Ref. [30], the duality is used to account for the extremely narrow decay width of pentaquark baryons[31, 32].

Hadrons in $SU(N)$ gauge theories are bound states of (anti-)quarks belonging to the (anti-)fundamental representation. In order to introduce such quarks and antiquarks, we need to place flavor D-branes in the dual gravity background[33]. Quarks are identified with endpoints of open strings on the flavor branes, and hadrons are constructed by connecting them. For example, a meson consisting of a quark and an antiquark is realized as an open string stretched between two flavor branes on the gravity side, as depicted in Fig. 1 (a).

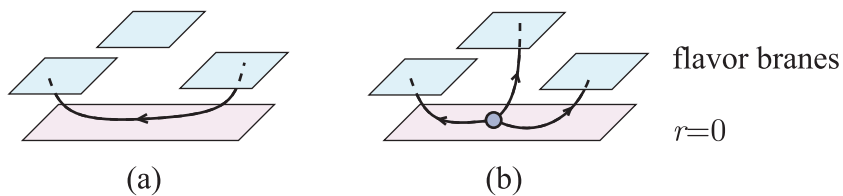


Figure 1: (a) A meson configuration and (b) a baryon configuration.

Among the many states in a meson spectrum, some low-lying states of pseudo-scalar and vector mesons are identified with string modes representing fluctuations of the flavor branes and gauge fields on them. The masses of such modes are examined in Refs. [9, 10], and the existence of localized modes with a mass gap is found in those works.

By contrast, Regge trajectories of higher-spin mesons can be treated as semi-classical spinning strings in curved backgrounds[9, 15]. In general, it is difficult to determine the motion of strings completely, and the Born-Oppenheimer approximation is often used to simplify such problems. In this method, a quark-antiquark

potential is computed as the energy of a string with fixed endpoints[34, 35], and then, the motion of the endpoints (the quark and the antiquark) is obtained by solving the resulting potential problem. If the distance L between a quark and an antiquark is large, the L dependence of the potential energy can in general be expanded as

$$E_{q\bar{q}} = TL + M_q + M_{\bar{q}} + \mathcal{O}(L^{-1}). \quad (1)$$

The coefficient T of the first term here is the tension of the confining string between the quark and the antiquark. From the gravity point of view, the first term is interpreted as the contribution from the tension of a fundamental string at $r = 0$, because fundamental strings tend to approach $r = 0$ as a result of the gravitational force. Thus, T is obtained as the product of the redshift (warp) factor and the proper tension of fundamental strings. In general, confining strings can be bound states of elementary confining strings. The tension of such strings depends non-linearly on the number of constituent elementary strings. This property is reproduced in the gravity description[36] by taking account of the effect of the transition of fundamental strings to D-branes expanded in internal spaces by Myers' effect[37]. The second and third terms in (1), which are independent of L , are interpreted as the self-energies of the quark and antiquark. These can be evaluated by analyzing the catenary profile of a string near flavor D-branes.

A baryon is constructed by connecting flavor D-branes with N open fundamental strings of the same orientation. In order to join such strings without violating the conservation law of the fundamental string charge, we have to introduce a baryon vertex at the joint[16, 5] (see Fig. 1 (b)). This baryon vertex is a certain D-brane wrapped around a non-trivial cycle in the internal space. In general, strings stretched between a baryon vertex and a flavor D-brane could be bound, and the number of confining strings meeting at a vertex can be smaller than N .

Let us consider the potential among quarks in a baryon in the spirit of the Born-Oppenheimer approximation.[17] If the length of each confining string is large, the energy of the baryon configuration is given by

$$E_{\text{baryon}} = \sum_i T_i L_i + \sum_i M_i + E_{\text{vertex}} + \mathcal{O}(L_i^{-1}), \quad (2)$$

where L_i and T_i are the length and the tension of the i -th confining string, and M_i represents the self-energy of the quark at the end of the i -th confining string. The third term, E_{vertex} , represents a new contribution which is absent in meson energies. Naively, this contribution can be evaluated by multiplying the tension T of the D-brane composing the baryon vertex, the volume V of the cycle around which the D-brane is wrapped, and the warp factor. Although this does not give an exact result, because of the deformation of the brane caused by the string tension[18, 19], we expect that a vertex gives some positive contribution of the order of $TV \times (\text{warp factor})$. The purpose of this work is to compute this quantity using both numerical and analytical methods.

This paper is organized as follows. In the next section, we describe the context we consider and clearly define the problem to be solved. The junctions are realized as D3-brane configurations embedded in a six-dimensional geometry. In §3, we briefly review the result of Ref. [36] concerning the confining string tension and study the kinematics of junctions associated with the tension balance. In §4, as preparation for the following computations, we rewrite brane configurations as two-dimensional surfaces in a certain four-dimensional target space by assuming a certain symmetry. The results of numerical computations are reported in §5, and we present analytic results in §6. We conclude in §7. In the appendix, we briefly explain how the electric fields on D3-branes are treated in the numerical computations.

2 D3-branes in the infrared geometry

We use two different classical solutions in type IIB supergravity as background spacetimes dual to $\mathcal{N} = 1$ supersymmetric confining gauge theories. One is the Maldacena-Núñez (MN) solution[38, 39], and the other is the Klebanov-Strassler (KS) solution[40, 41, 42].

The MN solution is the near horizon geometry of N coincident D5-branes wrapped around a two-cycle in a non-compact Calabi-Yau manifold. This is believed to be the gravity dual to the $\mathcal{N} = 1$ $SU(N)$ pure Yang-Mills theory. This theory has only two parameters, the size of the gauge group, N , and the confinement scale, Λ_{QCD} .

The KS solution can be interpreted as the near horizon geometry of $N + k$ coincident D5-branes and k anti-D5-branes wrapped around a two-cycle. The corresponding boundary field theory is an $\mathcal{N} = 1$ $SU(N+k) \times SU(k)$ gauge theory with bifundamental chiral multiplets. The number k depends on the energy scale. As the energy decreases, k also decreases due to cascade phenomenon[41]. In the brane picture, this can be regarded as a kind of pair annihilation of D5-branes and anti-D5-branes. At very low energy, all the anti-D5-branes disappear with the same number of D5-branes, leaving N D5-branes. Thus, the boundary theory of the KS solution behaves like the $\mathcal{N} = 1$ $SU(N)$ supersymmetric Yang-Mills theory in the low energy limit. In addition to N and Λ_{QCD} , this theory includes the parameter \bar{g} , defined by $\bar{g}^{-2} = g_1^{-2} + g_2^{-2}$, where g_1 and g_2 are the gauge coupling constants of $SU(N+k)$ and $SU(k)$, respectively. Although g_1 and g_2 run with the energy scale individually, \bar{g} is a renormalization invariant parameter. This parameter is related to the string coupling constant g_{str} , which is constant in the KS solution, as

$$\bar{g}^2 = 4\pi g_{\text{str}}. \quad (3)$$

Corresponding to the similarity of the types of low-energy behavior of the two gauge theories, the two classical solutions have similar structure. They are warped products of a five-dimensional manifold with coordinates (x^μ, r) and an

internal space with the topology $\mathbf{S}^2 \times \mathbf{S}^3$. \mathbf{S}^2 shrinks to a point at $r = 0$, while \mathbf{S}^3 possesses non-zero size everywhere. The infrared (IR) dynamics of the field theories are reflected by the structure near the centers of the classical solutions. For both the MN and the KS solutions, the metric of the $r = 0$ subspace relevant to the IR dynamics is given by

$$ds^2 = R^2(\eta_{\mu\nu}dy^\mu dy^\nu + d\Omega_3^2), \quad (\mu, \nu = 0, 1, 2, 3) \quad (4)$$

where $d\Omega_3^2$ is the metric of the unit 3-sphere. We refer to this as IR geometry. The size N of the low-energy gauge group $SU(N)$ of the boundary gauge theories is determined by the R-R 3-form flux flowing through \mathbf{S}^3 . In other words, the integral of the R-R 3-form field strength G_3 over the non-trivial 3 cycle gives N :

$$N = \oint_{\mathbf{S}^3} G_3. \quad (5)$$

The boundary theories of the MN and KS solutions include only adjoint and bifundamental fields. In order to introduce fundamental quarks into these theories, we need flavor D-branes. We can use D5[43, 12], D7[33, 10], or D9-branes[43] wrapped around appropriate cycles as flavor branes. Hadrons are constructed by connecting these branes with fundamental strings joined by baryon vertices. We assume that the lengths of the strings are large and focus on the vicinity of baryon vertices, which are located at the bottom ($r = 0$) of the classical solutions, due to the gravitational force. We do not discuss the effect of the endpoints of strings on the flavor branes, and the arguments given in this paper are independent of the choice of the flavor branes.

In the cases of the MN and KS backgrounds, baryon vertices are D3-branes wrapped around \mathbf{S}^3 [44, 40, 45], and fundamental strings in the IR geometry are expanded to D3-brane tubes with section \mathbf{S}^2 [36], due to the existence of the G_3 flux through Myers' effect[37]. Therefore, the junctions of the confining strings are dual to the D3-branes, with the electric flux on them embedded in the IR geometry.

The magnetic flux on D3-branes carries the charge of D-strings, which in the case of the KS solution have recently been identified with axionic strings[46, 47]. We do not consider them in this paper.

The action of a D3-brane in the IR geometry described by the metric (4) and the R-R flux (5) is

$$S = -T_{\text{D3}} \int d^4\sigma \sqrt{-\det\left(g_{ab} + \frac{2\pi}{T_{\text{str}}} F_{ab}\right)} + 2\pi \int F_2 \wedge C_2, \quad (a, b = 0, 1, 2, 3) \quad (6)$$

where $T_{\text{str}} = 1/(2\pi\alpha')$ and $T_{\text{D3}} = 1/((2\pi)^3\alpha'^2 g_{\text{str}})$ are the tensions of the fundamental strings and D3-branes, respectively. Also, C_2 is the R-R two-form potential and $G_3 = dC_2$. When a confining string consisting of n elementary strings is realized as a D3-brane configuration with the topology $\mathbf{R}^2 \times \mathbf{S}^2$, the

integer n is defined as the fundamental string charge carried by the D3-brane. The fundamental string current is derived from the action (6) by differentiating it with respect to the NS-NS two-form potential B_2 . (In the derivation of the current, F_2 should be regarded as the B -gauge invariant field strength $dA_1 + B_2$. Once we have obtained the current, we set $B_2 = 0$.) n is obtained by integrating the current as

$$n = - \oint_X dS_a D^a + \oint_X C_2 = - \oint_X dS_a D^a + \int_Y G_3, \quad (a = 1, 2, 3) \quad (7)$$

where X is a non-trivial 2-cycle in the D3-brane worldvolume, and Y is a 3-disk with boundary $\partial Y = X$. The flux density D^a in (7) is defined by

$$D^a = \frac{1}{2\pi} \frac{\delta S_{\text{BI}}}{\delta F_{0a}}. \quad (a = 1, 2, 3) \quad (8)$$

Note that we use S_{BI} , the Born-Infeld part of the action (6), to define D^a . The flux density defined in this way is invariant under gauge transformations of the R-R 2-form potential C_2 . Due to the ambiguity in the choice of Y in \mathbf{S}^3 , n is defined only mod N . n is a conserved charge and does not change under continuous deformations of the brane.

We define a ‘‘flux angle’’ θ^f by

$$\theta^f = \pi \frac{n}{N}, \quad (9)$$

for later use. We fix the mod- π ambiguity of θ^f by stipulating that $0 < \theta^f < \pi$. Because the sum of charges n of the strings meeting at a baryon vertex must be a multiple of N , the sum of the corresponding flux angles is a multiple of π . If there are three branches, the sum can be π or 2π . These two are essentially the same, due to the charge conjugation $\theta^f \rightarrow \pi - \theta^f$. If there are more than three branches there are more than two genuinely different cases, as we see below explicitly for four-string junctions.

To clarify the dependence of the action (6) on the parameters R and N , we factor these parameters out of the induced metric and the R-R 3-form flux, writing them as

$$g_{ab} = R^2 \tilde{g}_{ab}, \quad G_3 = \frac{N}{2\pi^2} \omega_3, \quad (10)$$

where ω_3 is the volume form of \mathbf{S}^3 normalized so that its integral over \mathbf{S}^3 gives $\oint_{\mathbf{S}^3} \omega_3 = 2\pi^2$, the volume of the unit 3-sphere. Next, we introduce a rescaled field strength \tilde{F}_2 and the corresponding potential \tilde{A}_1 as

$$F_2 = \frac{R^2 T_{\text{str}}}{2\pi} \tilde{F}_2, \quad A_1 = \frac{R^2 T_{\text{str}}}{2\pi} \tilde{A}_1. \quad (11)$$

The D3-brane action rewritten in terms of these rescaled fields is

$$\tilde{S} = - \int d^4\sigma \sqrt{-\det(\tilde{g}_{ab} + \tilde{F}_{ab})} + \rho \int \tilde{A}_1 \wedge \omega_3, \quad \rho = \frac{N T_{\text{str}}}{2\pi^2 R^2 T_{\text{D3}}}. \quad (12)$$

Here, we have changed the normalization of the action from S to \tilde{S} , which are related by $S = T_{\text{D3}} R^4 \tilde{S}$. This does not affect the classical equations of motion in which we are interested. The dimensionless quantity ρ is the unique parameter of this rescaled action. It is related to the parameter b used in Ref. [36] by $\rho = 2/b$. Also note the relation

$$\frac{2}{\rho} = b = \frac{R^2}{R_{\text{D5}}^2}, \quad (13)$$

where $R_{\text{D5}} = (N\alpha' g_{\text{str}})^{1/2}$ is the radius of \mathbf{S}^3 near the horizon of N coincident flat D5-branes in the flat Minkowski background. Because the MN solution can be regarded as the near horizon geometry of D5-branes wrapped around \mathbf{S}^2 , the radius R is identical to R_{D5} , and $b = 1$. However, for the KS solution, b is modified due to the existence of anti D5-branes, and its numerical value is $b = 0.932660368 \dots$ [41, 36]. From the action (12), it is seen that we can regard the dimensionless parameter ρ as a charge density coupled to the gauge field \tilde{A}_1 .

In this paper, we only consider static configurations, and we always omit the time dimension in the following. By the term ‘‘worldvolume’’ we refer to a time slice of the entire worldvolume.

Instead of D^a defined by (8), we use the rescaled flux density and its Hodge dual defined by

$$\tilde{D}^a = \frac{\delta \tilde{S}}{\delta \tilde{F}_{0a}} = \frac{2\pi^2 \rho}{N} D^a, \quad \tilde{D}_2 = \frac{1}{2} \sqrt{\det \tilde{g}_{ab}} \epsilon_{abc} D^a d\sigma^b \wedge d\sigma^c. \quad (a, b, c = 1, 2, 3) \quad (14)$$

The relation (7) rewritten in terms of the flux angle and the rescaled flux density becomes

$$2\pi\rho\theta^f = - \oint_X \tilde{D}_2 + \rho \int_Y \omega_3. \quad (15)$$

This is the integral form of the Gauss’s Law constraint,

$$d\tilde{D}_2 = \rho\omega_3|_{\text{brane}}, \quad (16)$$

where $\omega_3|_{\text{brane}}$ is the pull-back of ω_3 to the D3-brane worldvolume.

The energy of a D3-brane is given by $E = T_{\text{D3}} R^3 \tilde{E}$ where \tilde{E} is the rescaled energy

$$\tilde{E} = \int d^3\sigma \sqrt{\det \tilde{g}_{ab}} \sqrt{1 + \tilde{g}_{ab} \tilde{D}^a \tilde{D}^b}. \quad (a, b = 1, 2, 3) \quad (17)$$

The shape of a D3-brane and the electric flux density on it should be determined so that energy is minimized.

In the following sections, we use only rescaled quantities, such as \tilde{E} , \tilde{D}^a and \tilde{g}_{ab} . In the rest of this section, we summarize the relations between these dimensionless quantities and dimensionful quantities in boundary field theories. From the definition of the rescaled quantities \tilde{S} and \tilde{g}_{ab} , we can determine the relations between the rescaled energies and tensions and original ones. To determine

the corresponding quantities in boundary field theories, we should also take account of the warp factor W , which determines the ratio of the energies in the IR geometry and those in the boundary field theories. Doing this, we obtain

$$E_{\text{vertex}}^{(\text{FT})} = WT_{D3}R^3\tilde{E} = \left(\frac{W}{\alpha^{1/2}}\right) \frac{bN^{3/2}g_{\text{str}}^{1/2}}{(2\pi)^3}\tilde{E}_{\text{vertex}}, \quad (18)$$

$$T^{(\text{FT})} = W^2T_{D3}R^2\tilde{T} = \left(\frac{W}{\alpha^{1/2}}\right)^2 \frac{bN}{(2\pi)^3}\tilde{T}, \quad (19)$$

where $\tilde{E}_{\text{vertex}}$ and \tilde{T} are the energy of a baryon vertex and a confining string tension, given in the following sections, and $E_{\text{vertex}}^{(\text{FT})}$ and $T^{(\text{FT})}$ are the corresponding quantities in the boundary field theories.

The confinement scale Λ_{QCD} in the boundary gauge theories can be defined by $T^{(\text{FT})} \sim \Lambda_{\text{QCD}}^2$. Thus, up to a numerical factor, we have

$$\Lambda_{\text{QCD}} \sim \frac{W}{\alpha^{1/2}}. \quad (20)$$

(Here we have used the tension of an elementary confining string, $\tilde{T} \sim N^{-1}$.) Then, the energy of a baryon vertex can be rewritten as

$$E_{\text{vertex}}^{(\text{FT})} \sim \Lambda_{\text{QCD}}N^{3/2}g_{\text{str}}^{1/2}\tilde{E}_{\text{vertex}}. \quad (21)$$

This depends on the string coupling constant, g_{str} . In the KS case, g_{str} is related to the parameter \bar{g} by (3), and we obtain the following relation, which includes only field theory variables:

$$E_{\text{vertex}}^{(\text{FT})} \sim \Lambda_{\text{QCD}}N^{3/2}\bar{g}\tilde{E}_{\text{vertex}}. \quad (22)$$

By contrast, there is no parameter corresponding to g_{str} in the MN case. We return to this problem in §6.

In the following sections, we use only dimensionless quantities, and we omit the tildes on rescaled variables for simplicity.

3 Confining strings and their junctions

In this section we first briefly review how the tensions of confining strings are computed as the energies of D3-branes, following Ref. [36]. Next, we study the kinematics of junctions by considering the balance of tensions on vertices.

Let (x, y, z) be the three spatial coordinates of the boundary. Combining these with the coordinates of the internal space \mathbf{S}^3 , we have the set of coordinates $(x, y, z, \theta, \phi, \psi)$ with the following metric:

$$ds^2 = dx^2 + dy^2 + dz^2 + d\theta^2 + \sin^2\theta(d\phi^2 + \sin^2\phi d\psi^2). \quad (23)$$

The ranges of the angular coordinates are

$$0 \leq \theta \leq \pi, \quad 0 \leq \phi \leq \pi, \quad 0 \leq \psi < 2\pi. \quad (24)$$

With this parameterization, the volume form of \mathbf{S}^3 is given by

$$\omega_3 = \sin^2 \theta \sin \phi d\theta \wedge d\phi \wedge d\psi. \quad (25)$$

The dual configuration of an infinitely long confining string is a D3-brane with the worldvolume $\mathbf{S}^2 \times \mathbf{R}$. We begin with the ansatz

$$x = \sigma^1, \quad y = 0, \quad z = 0, \quad \theta = \theta^r, \quad \phi = \sigma^2, \quad \psi = \sigma^3. \quad (26)$$

The parameter θ^r is a constant representing the angular radius of $\mathbf{S}^2 \subset \mathbf{S}^3$. By rotational symmetry, we can easily determine the flux density D^a as a function of θ^f and θ^r from (15). Its only non-vanishing component is D^x , and it is given explicitly by

$$D^x = \frac{-1}{b \sin^2 \theta^r} [\theta^f - (\theta^r - \sin \theta^r \cos \theta^r)]. \quad (27)$$

Substituting this into (17), we obtain the tension of a confining string.

$$T = \frac{dE}{dx} = 4\pi \sqrt{\sin^4 \theta^r + \frac{1}{b^2} (\theta^f - \theta^r + \sin \theta^r \cos \theta^r)^2}. \quad (28)$$

We should determine the angle θ^r as the point of minimum tension. The condition $dT/d\theta^r = 0$ gives the relation between θ^f and θ^r ,

$$\theta^r - (1 - b^2) \sin \theta^r \cos \theta^r = \theta^f. \quad (29)$$

If $0 \leq b^2 \leq 1$, this relation defines a one to one mapping between $0 \leq \theta^f \leq \pi$ and $0 \leq \theta^r \leq \pi$. The minimum value of the tension is

$$T = 4\pi \sin \theta^r \sqrt{\sin^2 \theta^r + b^2 \cos^2 \theta^r}. \quad (30)$$

For the MN solution, (29) can be solved immediately, and the tension (30) reduces to the simple form

$$\theta^f = \theta^r, \quad T = 4\pi \sin \theta^f, \quad \text{for } b = 1. \quad (31)$$

Contrastingly, the angle θ^r and the tension for the KS solution can only be obtained numerically. The tensions T and angles θ^r for several values of θ^f are listed in Table 1. These values are used below to compute the energies of the baryon vertices.

In the cases of both the MN and KS backgrounds, the tension depends non-linearly on θ^f . This non-linear dependence implies the formation of truly bound states and the absence of supersymmetry. Therefore we cannot apply the method

Table 1: The angle θ^r and the tension T for several values of θ^f

θ^f	MN ($b = 1$)		KS ($b = 0.9326604$)	
	θ^r	T	θ^r	T
$\pi/12 = 0.261799$	0.261799	3.252416	0.298366	3.467446
$2\pi/12 = 0.523599$	0.523599	6.283185	0.583434	6.601513
$3\pi/12 = 0.785398$	0.785398	8.885766	0.849929	9.168758
$4\pi/12 = 1.047198$	1.047198	10.882796	1.099822	11.047175
$5\pi/12 = 1.308997$	1.308997	12.138181	1.338189	12.185588
$6\pi/12 = 1.570796$	1.570796	12.566371	1.570796	12.566371

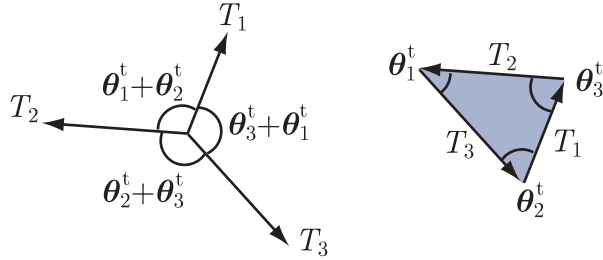


Figure 2: The balance of three tensions.

employing Killing spinors, which is useful to determine the baryon configuration in $\mathcal{N} = 4$ Yang-Mills theory[18], to configurations investigated in this paper.

Using the tension formula obtained above, we now consider the kinematics of three- and four-string junctions. We first study three-string junctions. The angles at which the strings meet are fixed by the requirement that of the tensions balance at the vertex. If we define the angle θ_i^t as the angle opposite the force vector of the i -th string in the triangle consisting of three force vectors, the angle made by the i -th and j -th strings is $\theta_i^t + \theta_j^t$ (see Fig. 2). If the tensions of the three strings are T_i , $i = 1, 2, 3$, the angles are uniquely determined by

$$\theta_1^t = \cos^{-1} \frac{T_2^2 + T_3^2 - T_1^2}{2T_2T_3}, \quad 0 < \theta_1^t < \pi, \quad (32)$$

and similar equations for θ_2^t and θ_3^t . These are equivalent to the following:

$$T_1 : T_2 : T_3 = \sin \theta_1^t : \sin \theta_2^t : \sin \theta_3^t, \quad \theta_1^t + \theta_2^t + \theta_3^t = \pi. \quad (33)$$

Unlike the relation between θ_i^f and θ_i^r , θ_i^t is not a function of only the single angle θ_i^f with the same index i . Rather, it is a function of the set of angles $\{\theta_1^f, \theta_2^f, \theta_3^f\}$. Because the sum of the three flux angles is π or 2π , only two of them are independent. We represent θ_1^t as a function of θ_2^f and θ_3^f and denote it by

$\theta_1^t = \tau(\theta_2^f, \theta_3^f)$. The other two angles are similarly given by $\theta_2^t = \tau(\theta_3^f, \theta_1^f)$ and $\theta_3^t = \tau(\theta_1^f, \theta_2^f)$, with the same function τ .

For the MN case, (33) reduces to the simple relation $\sin \theta_i^t = \sin \theta_i^f$. Even in this case, we cannot determine θ_i^t from only the single angle θ_i^f , because there are two solutions, $\theta_i^t = \theta_i^f$ and $\theta_i^t = \pi - \theta_i^f$. These two solutions correspond to the two possible values π and 2π of the total flux angle, $\theta_{\text{tot}}^f = \sum_{i=1}^3 \theta_i^f$, respectively. These two cases can be expressed together by the single equation

$$\theta_3^t = \tau(\theta_1^f, \theta_2^f) = |\pi - \theta_1^f - \theta_2^f|. \quad (34)$$

We now proceed to consider four-string junctions. We assume that the four external strings are on a plane. We label the external strings in counterclockwise order by 1, 2, 3 and 4, and denote the angle made by strings i and $i+1$ by $\theta_{i,i+1}$. [see Fig. 3 (a)] (The labels of the strings are defined mod 4.) The sum of these

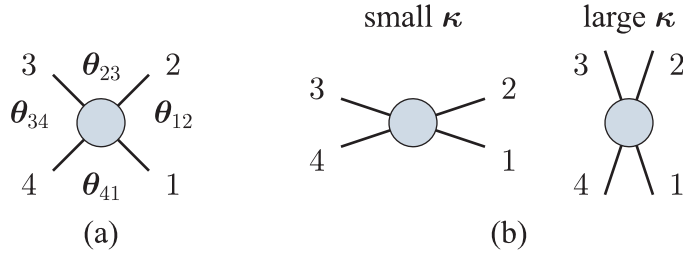


Figure 3: A junction with four external strings.

four angles is 2π , and only three of them are independent. If the flux angles $\{\theta_1^f, \theta_2^f, \theta_3^f, \theta_4^f\}$ of the four branches are given, the tensions are determined by the formula above, and the balance of these four tensions imposes two conditions on the angles $\theta_{i,i+1}$. These conditions leave one degree of freedom unfixed. We define a parameter κ parameterizing this unfixed degree of freedom. One useful choice is

$$\kappa = \theta_{12} + \theta_{34} = 2\pi - (\theta_{23} + \theta_{41}). \quad (35)$$

If this parameter changes, the junction deforms as in Fig. 3(b).

There are three possible topologies of four-string junctions, as shown in Fig. 4. For junctions with the topologies (H) and (I), which include two three-string vertices, the angles $\theta_{i,i+1}$ are uniquely determined by the flux angles, and the corresponding κ -parameters are given by

$$\kappa_H = 2\pi - \tau(\theta_1^f, \theta_2^f) - \tau(\theta_3^f, \theta_4^f), \quad \kappa_I = \tau(\theta_2^f, \theta_3^f) + \tau(\theta_4^f, \theta_1^f). \quad (36)$$

Let us suppose that there is a junction with the topology (H). This can be in equilibrium if $\kappa = \kappa_H$. If we try to change the parameter κ by changing the directions of the strings, the two vertices move in such a way that the movement compensates for the variation of κ . If we attempt to decrease κ , two vertices move

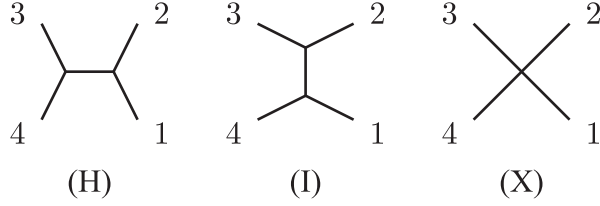


Figure 4: The three possible topologies of four-string junctions. Two of them include two three-string vertices and the other has one four-string vertex.

away from each other, with the result that κ remains unchanged. If we move the strings in the opposite direction, the two vertices approach each other. This compensating mechanism consisting of the movement of vertices is effective until the two vertices coincide. If we continue to move the strings after the vertices come to coincide, the topology of the junction tends to change to (I) via (X). Until the instant at which the two vertices first coincide, we have $\kappa = \kappa_H$, and the behavior of the junction after this instant depends on the relation between κ_H and κ_I .

If $\kappa_H > \kappa_I$, just as the two vertices of (H) meet, the topology of the junction changes to (I) and becomes unstable, and then the two vertices separate rapidly, eventually realizing the equilibrium condition, $\kappa = \kappa_I$. In this case, the junctions of the topology (X) are unstable.

If $\kappa_H < \kappa_I$, even after the two vertices coincide, the topology does not change to (I), and (X) is stable until κ reaches κ_I . When κ reaches κ_I , the topology of the junction finally changes to (I).

When $\kappa_H = \kappa_I$, there is a unique value of κ that gives stable configurations, and the three topologies can change to each other marginally without changing κ .

To express these types of behavior of the junctions, it is convenient to define the parameter $\lambda \equiv \kappa_H - \kappa_I$ representing the “repulsive force” between two vertices. If λ is positive, two three-string vertices repel each other, and they cannot merge to form a stable four-string vertex. If λ is negative, two vertices attract each other, and they are bound into a four-string vertex, provided that $\kappa_H < \kappa < \kappa_I$.

Which cases are realized for junctions in the MN and KS backgrounds? From (35) and (36), $\lambda = \kappa_H - \kappa_I$ is given by

$$\lambda = 2\pi - \tau(\theta_1^f, \theta_2^f) - \tau(\theta_2^f, \theta_3^f) - \tau(\theta_3^f, \theta_4^f) - \tau(\theta_4^f, \theta_1^f). \quad (37)$$

For the MN solution, the explicit form of λ is

$$\lambda = 2\pi - |\pi - \theta_1^f - \theta_2^f| - |\pi - \theta_2^f - \theta_3^f| - |\pi - \theta_3^f - \theta_4^f| - |\pi - \theta_4^f - \theta_1^f|. \quad (38)$$

We can easily show that $\lambda = 0$ when $\sum_{i=1}^4 \theta_i^f = \pi$ or $\sum_{i=1}^4 \theta_i^f = 3\pi$ and that $\lambda > 0$ when $\sum_{i=1}^4 \theta_i^f = 2\pi$.

For the KS solution, although it is difficult to determine the signature of λ analytically, we can numerically check that it is always positive. This implies that planar four-string junctions are always unstable in the KS background.

4 Reduction to lower dimensions

In the last section, we saw that junctions are described as three-dimensional surfaces in the six-dimensional space spanned by the coordinates $(x, y, z, \theta, \phi, \psi)$. We only consider planar junctions and set $z = 0$. If we ignore the extension along the (x, y) -plane, the worldvolume of a D3-brane representing a k -string junction is \mathbf{S}^3 with k punctures. Each puncture is topologically a three-dimensional disc and corresponds to each branch string. Let us assume that these punctures are located on a large circle of \mathbf{S}^3 . In this case, the configuration possesses U(1) symmetry, as determined by the symmetry group of this circle. It is convenient to choose \mathbf{S}^1 given by $g_{\psi\psi} = 0$ as the fixed large circle so that the U(1) action constitutes a constant shift of the coordinate ψ . General brane configurations with this U(1) symmetry are

$$x = x(\sigma^1, \sigma^2), \quad y = y(\sigma^1, \sigma^2), \quad \theta = \theta(\sigma^1, \sigma^2), \quad \phi = \phi(\sigma^1, \sigma^2), \quad \psi = \sigma^3. \quad (39)$$

Thus, we can represent configurations as two-dimensional surfaces in the four-dimensional space with the coordinates (x, y, θ, ϕ) .

Instead of the angular coordinates (θ, ϕ) , it is convenient to use (u, v, w) satisfying constraints $u^2 + v^2 + w^2 = 1$ and $w \geq 0$. The relations among these coordinates are

$$u = \sin \theta \cos \phi, \quad v = \cos \theta, \quad w = \sin \theta \sin \phi \quad (40)$$

(see Fig. 5). If we use (x, y, u, v) as a set of independent coordinates, the target space is $\mathbf{R}^2 \times \mathbf{D}^2$, where \mathbf{R}^2 is spanned by x and y , and \mathbf{D}^2 is the unit disc satisfying $u^2 + v^2 \leq 1$ in the (u, v) -plane. The variable $w = \sqrt{1 - u^2 - v^2}$ is treated as a function of u and v . Brane configurations are two-dimensional surfaces embedded in this four-dimensional target space. For example, a confining string solution given in §3 is represented as a band in the four-dimensional space which is a direct product of a chord $v = \cos \theta^r$ on the unit disc and an infinitely long line in the (x, y) -plane.

We should redefine the electric flux density as a field on the two-dimensional surface by integrating the flux density D_2 over ψ . We introduce a one-form D'_1 and its dual vector D'^a as

$$D'_1 = \int_{\psi} D_2, \quad D'_1 = \sqrt{\det g_{ab}} \epsilon_{ab} D'^a d\sigma^b. \quad (a, b = 1, 2) \quad (41)$$

The Gauss's Law constraint satisfied by D'_1 is obtained by integrating the constraint (16) given by

$$dD'_1 = 2\pi \rho du \wedge dv. \quad (42)$$

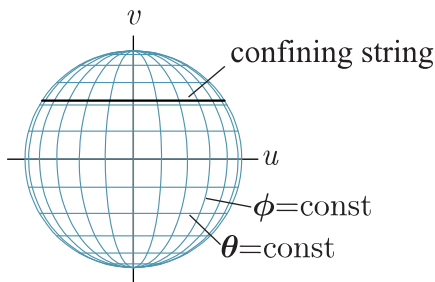


Figure 5: The projection of the hemisphere parameterized by (θ, ϕ) onto the unit disc in the (u, v) -plane. The cross-section of a confining string solution is represented as a chord of this unit circle in the (u, v) -plane.

The corresponding integral form is

$$2\pi\rho\theta^f = - \oint_C D'_1 + 2\pi\rho \int_A du \wedge dv, \quad (43)$$

where C and A correspond to X and Y in (15), respectively. C is a curve on the surface connecting two boundaries. A is a two-dimensional surface whose boundary consists of C and a curve in the boundary $u^2 + v^2 = 1$ of the four-dimensional target space. To obtain the right-hand sides of Eqs. (42) and (43), we have used the relation

$$\int_\psi \omega_3 = 2\pi \sin^2 \theta \sin \phi d\theta \wedge d\phi = 2\pi du \wedge dv. \quad (44)$$

The energy (17) integrated over ψ is

$$E = \int d^2\sigma \sqrt{\det g_{ab}} \sqrt{(2\pi w)^2 + g_{ab} D'^a D'^b}. \quad (a, b = 1, 2) \quad (45)$$

Now, the problem that we wish to solve is to find a two-dimensional surface in the four-dimensional space (x, y, u, v) and a flux density D'_1 on it which minimize the energy (45) under the constraint (43) imposed on each external confining string.

When we perform a numerical computation to determine a brane configuration, we start from an initial configuration and look for a configuration with minimum energy by varying the shape of the surface and the flux on it. We can choose any configuration as the initial configuration, as long as it satisfies appropriate boundary conditions and (43), and as long as it is in the same topological class as the final configuration we wish to obtain. One natural choice for a confining string is a D3-brane with a shrunk worldvolume, for which the second term of (15) vanishes. This represents a brane before being expanded by Myers' effect. This choice, however, is very singular and not appropriate for the numerical computation. Therefore, we instead adopt a worldvolume on which

the electric flux density vanishes everywhere on the surface. In this case, the constraint (43) requires that the area in the (u, v) -plane enclosed by C and the unit circle $u^2 + v^2 = 1$ be the same as the flux angle θ^f . The most convenient one satisfying this condition is the “wedge configuration” defined as a direct product of a line in the (x, y) -plane and a wedge in the (u, v) -plane, as shown in Fig. 6 (a).

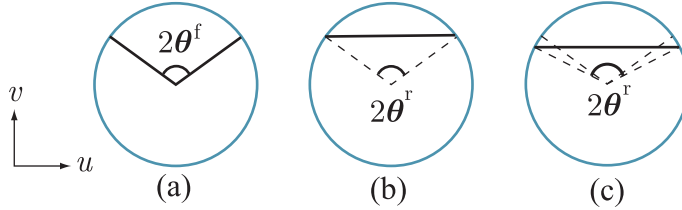


Figure 6: The projections of brane configurations in the (u, v) -plane. (a) The wedge configuration used as an initial configuration. (b), (c) The confining string solutions in the MN and KS backgrounds, respectively.

Starting from a wedge configuration with a central angle $2\theta^f$, we can numerically reproduce the corresponding confining string solution represented as a chord in the (u, v) -plane. Its length is determined by θ^r defined in §3. For the MN solution, the two angles θ^f and θ^r are equal. This implies that the distance between the two endpoints of the wedge on the unit circle is the same as the length of the chord [see Fig. 6 (b)]. However, this distance becomes slightly greater for the KS solution. [see Fig. 6 (c)].

Wedge configurations are also suitable to construct initial configurations for junctions, because they can be pasted just like interaction vertices in Witten’s open string field theory[48], as shown in Fig. 7 (a). By varying this initial

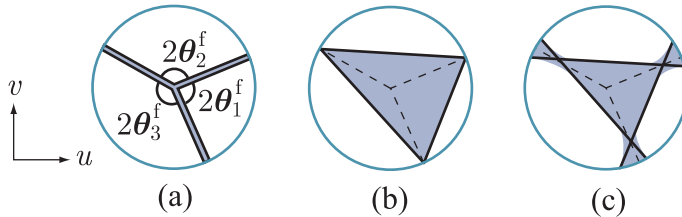


Figure 7: (a) An initial configuration for a three string junction is composed of three wedge configurations. After minimizing the energy by varying the configuration, we obtain the junction solutions for (b) the MN background and (c) the KS background, respectively.

configuration and minimizing the energy, we obtain a junction configuration.

In the case of the MN background, the distance between the endpoints of each curve representing each branch string does not change, and the junction solution

is expected to be a triangle inscribed in the unit circle in the (u, v) -plane [see Fig. 7 (b)]. Indeed, the coincidence of the endpoints of the three chords is guaranteed by the relations (53), given below. It is important that this triangle is similar to the tension triangle in Fig. 2.

For the KS solution, the chords representing asymptotic string solutions are too long to make an inscribed triangle [see Fig. 7 (c)].

5 Numerical analysis

In this section, we report our results of our numerical study of brane configurations. We start by reconstructing the confining string solutions to assess the accuracy of the results of the numerical method by comparing them to the analytic results given in §3.

We first prepare a wedge configuration with a central angle $2\theta^f$ and a length L as an initial configuration [see Fig. 8 (a)]. We compute the energy of the surface by means of the triangulation method. The surface is divided into a

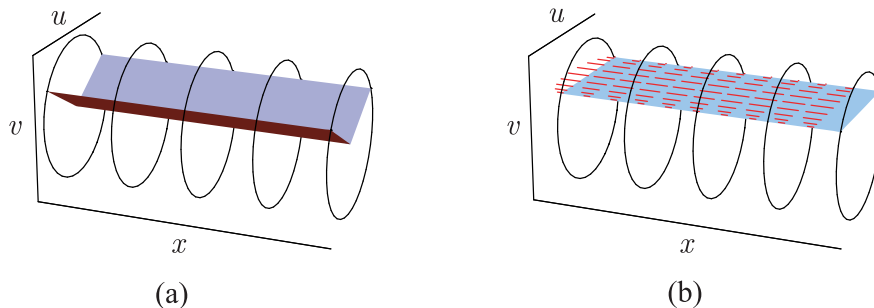


Figure 8: (a) An initial wedge configuration and (b) a numerically generated confining string solution. The segments in the worldvolume in (b) represent the flux density.

mesh of $2n_{\text{mesh}}^2$ small triangular regions. The shape of the surface is represented by the positions of the sites, and the flux density is treated as link variables. We seek a configuration that minimizes the energy by varying these variables while enforcing the Gauss's Law constraint. The detailed algorithm is given in the appendix. A result for $(\theta^f = \pi/3, L = 4, b = 1)$ is given in Table 2. By comparing this result to the corresponding tension in Table 1, we can estimate the accuracy of the outputs of the numerical analysis. We find a relative error of order $\sim 10^{-4}$ for the finest meshes, with $n_{\text{mesh}} \sim 80$. Plotting the error as a function of the typical size of triangles, $a = n_{\text{mesh}}^{-2}$, we find that the error is almost proportional to a (see Fig. 9). The value for $n_{\text{mesh}} = \infty$ ($a = 0$) given in Table 2 is obtained by extrapolating the data for finite n_{mesh} with a polynomial of a . This extrapolation gives a value very close to the exact one, with a relative error

Table 2: A numerical result for the tension of a confining string with $\theta^f = \pi/3$ in the MN solution. The value for $n_{\text{mesh}} \rightarrow \infty$ is obtained by extrapolating the data for $n_{\text{mesh}} = 10, 20, 40$ and 80 with the fitting function $c_0 + c_1 n_{\text{mesh}}^{-2} + c_2 n_{\text{mesh}}^{-4} + c_3 n_{\text{mesh}}^{-6}$.

n_{mesh}	10	20	40	80	∞	exact
$T = E/L$	10.7858	10.85978	10.87722	10.88144	10.88283	10.88280
error	-0.0970	-0.02302	-0.00558	-0.00136	+0.00003	-

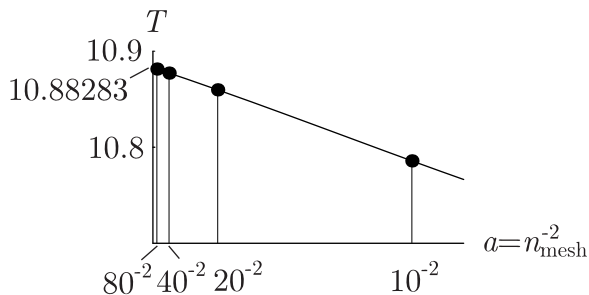


Figure 9: A fitting of numerically generated tensions for several values n_{mesh} .

$< 10^{-5}$. Because of this small error, we use the same extrapolation to obtain the energies of the baryon vertices.

Let $E_{\text{junc}}(L)$ be the energy of a three string junction with the branch length L . Then, the contribution from a baryon vertex is defined by

$$E_{\text{vertex}} = \lim_{L \rightarrow \infty} \left(E_{\text{junc}}(\theta_i^f, L) - L \sum_i T(\theta_i^f) \right). \quad (46)$$

However, we cannot in practice numerically compute E_{junc} in the limit $L \rightarrow \infty$. Therefore, instead, we use a sufficiently long fixed length beyond which the effect of the vertices becomes negligible. In the following way, we find evidence that $L = 4$ is sufficiently large to guarantee a relative accuracy of 10^{-5} . First, we compute the energies of two strings stretched between $x = 0$ and $x = L$ with lengths $L = 4$ and $L = 8$. The worldvolume of the short and the long strings are composed of $2n_{\text{mesh}}^2$ and $4n_{\text{mesh}}^2$ triangles, respectively. Hence the areas of the triangles are almost the same. The difference between the present computation and that described above to estimate the accuracy is that here on one boundary at $x = 0$ we impose a fixed boundary condition that prohibits the shape of the boundary from changing from a wedge to a straight chord. Thus, the resulting configurations have a wedge-shaped boundary at $x = 0$, and as x becomes large, the shape approaches a string solution (see Fig. 10). If the difference in energy between the two branes of lengths $L = 4$ and 8 is sufficiently close to the energy of a confining string of length $4 = 8 - 4$, we judge the configuration to be sufficiently

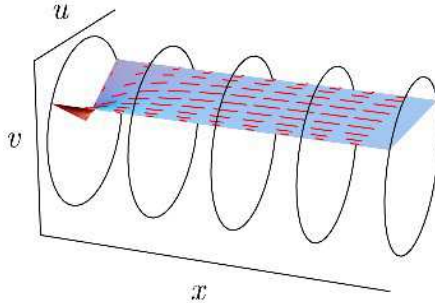


Figure 10: The brane configuration with a boundary on which the fixed boundary condition is imposed.

close to the string solution around $x \sim 4$, and we can use $L = 4$ to compute the energies of the baryon vertices. The result of this analysis is given in Table

Table 3: The numerically computed energies of the confining string configurations with a fixed boundary at one end. $T(n_{\text{mesh}})$ is the numerically computed tension given in Table 2.

n_{mesh}	10	20	40	80
$E_{L=8}$	87.2002	87.75829	87.88710	87.91770
$E_{L=4}$	44.0562	44.31901	44.37818	44.39194
$(E_{L=8} - E_{L=4})/(8 - 4)$	10.7860	10.85982	10.87723	10.88144
Difference from $T(n_{\text{mesh}})$	+0.0002	+0.00004	+0.00001	+0.00000

3. There it is seen that indeed the configuration is sufficiently close to a string solution before x reaches $L = 4$.

Based on the above preliminary results, we can finally compute the energies of the baryon vertices. The initial configurations are combinations of three wedges pasted like Witten's 3-string vertices [see Fig. 11 (a)]. The directions of three branches of initial configurations in the (x, y) -plane are set as in Fig. 2, so that the tensions are balanced. Now, instead of taking the $L \rightarrow \infty$ limit, we simply use $L = 4$, and each branch consists of $2n_{\text{mesh}}^2$ triangles.

We give the results for the KS background in Table 4. Because vertices with more than three branches are unstable, we only give the results for three string vertices. Contrary to the intuitive expectation, the signatures of the baryon vertex energies are negative. Their absolute values depend on the ratio of the flux angles, and it seems that the energy becomes closer to zero as the flux angles become increasingly asymmetric. This behavior was expected because in the limit that one of the flux angles vanishes, the junction becomes a confining string configuration, and the energy of the vertex goes to zero.

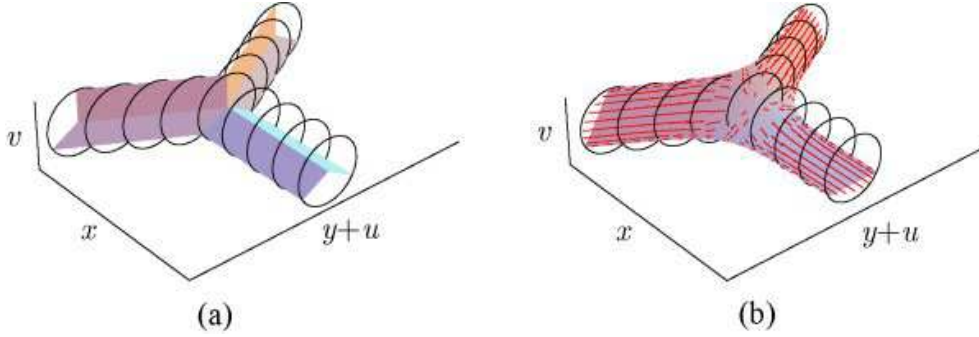


Figure 11: An initial configuration composed of three wedge configurations and the corresponding final junction configuration obtained numerically.

Table 4: The energies of baryon vertices in the KS solution. E_{junc} is the energy of an entire junction of branch length $L = 4$. E_0 represents the contribution of branches, computed as $E_0 = \sum_{i=1}^3 LT(\theta_i^f)$. The energy of a vertex is defined by $E_{\text{vertex}} = E_{\text{junc}} - E_0$. The shaded numbers are the final results obtained by extrapolation.

$(\theta_1^f, \theta_2^f, \theta_3^f)$	n_{mesh}	10	20	40	80	∞
$(\frac{4\pi}{12}, \frac{4\pi}{12}, \frac{4\pi}{12})$	E_{junc}	131.014	131.8324	132.0261	132.0731	132.0886
$E_0 = 132.5661$	E_{vertex}	-1.552	-0.7337	-0.5400	-0.5130	-0.4775
$(\frac{3\pi}{12}, \frac{4\pi}{12}, \frac{5\pi}{12})$	E_{junc}	128.126	128.9356	129.1274	129.1740	129.1894
$E_0 = 129.6061$	E_{vertex}	-1.480	-0.6705	-0.4787	-0.4321	-0.4167
$(\frac{2\pi}{12}, \frac{5\pi}{12}, \frac{5\pi}{12})$	E_{junc}	122.473	123.3349	123.5420	123.5927	123.6095
$E_0 = 123.8908$	E_{vertex}	-1.418	-0.5559	-0.3488	-0.2981	-0.2813

The results for the vertex energies in the MN background are more interesting. As shown in Table 5, the ratios of the vertex contributions to the total energies are smaller than 10^{-5} . This strongly suggests that the energies of baryon vertices exactly vanish for any values of the flux angles. In other words, the energy of a junction is obtained by summing up the contribution of each branch given as the product of its tension and its length in the (x, y) -plane. In Table 6, we give another result for a stable planar four-string vertex. It too seems consistent with a vanishing vertex energy.

Before ending this section, we confirm that junction configurations in the MN background have the asymptotic forms suggested in §3, which are represented as triangles in the (u, v) -plane. The projection of a numerically generated junction in the (u, v) -plane is shown in Fig. 12, and it indeed seems to be a triangle, as expected.

Table 5: The energies of baryon vertices in the MN solution. E_{junc} , E_0 , and E_{vertex} are defined in the same way as those in Table 4. The shaded numbers are the final results obtained by extrapolation.

$(\theta_1^f, \theta_2^f, \theta_3^f)$	n_{mesh}	10	20	40	80	∞
$(\frac{4\pi}{12}, \frac{4\pi}{12}, \frac{4\pi}{12})$	E_{junc}	129.584	130.3545	130.5356	130.5794	130.5939
$E_0 = 130.5936$	E_{vertex}	-1.010	-0.2391	-0.0580	-0.0142	+0.0003
$(\frac{3\pi}{12}, \frac{4\pi}{12}, \frac{5\pi}{12})$	E_{junc}	126.616	127.3866	127.5686	127.6127	127.6273
$E_0 = 127.6270$	E_{vertex}	-1.011	-0.2404	-0.0584	-0.0143	+0.0003
$(\frac{2\pi}{12}, \frac{5\pi}{12}, \frac{5\pi}{12})$	E_{junc}	121.116	121.9670	122.1716	122.2217	122.2383
$E_0 = 122.2382$	E_{vertex}	-1.122	-0.2712	-0.0666	-0.0165	+0.0001

Table 6: The energy of a planar four-string vertex with $\theta_i^f = \pi/4$. E_{junc} , E_0 , and E_{vertex} are defined in the same way as those in Table 4 and 5. The shaded number is the final result obtained by extrapolation.

$(\theta_1^f, \theta_2^f, \theta_3^f, \theta_4^f)$	n_{mesh}	10	20	40	80	∞
$(\frac{3\pi}{12}, \frac{3\pi}{12}, \frac{3\pi}{12}, \frac{3\pi}{12})$	E_{junc}	141.329	141.9459	142.1079	142.1537	142.1695
$E_0 = 142.1723$	E_{vertex}	-0.843	-0.2264	-0.0644	-0.0186	-0.0028

6 Analytic proof

As we saw in the last section, the numerical results for junctions in the MN background strongly suggest that baryon vertices do not contribute to the energies of junctions. This is also the case for supersymmetric junctions consisting of (p, q) -strings. [49, 50, 51, 52, 53, 54, 55] This fact for (p, q) -junctions is proven by dualizing junctions to membrane configurations in M-theory[54]. From this viewpoint, junctions are represented as two-dimensional smooth surfaces embedded in a four-dimensional space $\mathbf{R}^2 \times \mathbf{T}^2$. Let (X, Y) and (U, V) be orthogonal coordinates in \mathbf{R}^2 and \mathbf{T}^2 , respectively. We combine them into two complex coordinates, $Z_1 = X + iU$ and $Z_2 = Y + iV$. Then, a surface in this space is represented by a function $Z_2 = F(Z_1, \bar{Z}_1)$. It is known that if we require a brane configuration to be supersymmetric, the function F must be holomorphic[54, 55]. This fact is very important in proving the disappearance of the energies of vertices[54].

Brane configurations in the MN background have a similar property. As we have seen, they are described as two-dimensional smooth open surfaces in the four-dimensional space $\mathbf{R}^2 \times \mathbf{D}^2$ with coordinates (x, y, u, v) . Let us define complex coordinates $z_1 = x + iu$ and $z_2 = y + iv$ in analogy to the (p, q) -junction case. A surface can be represented by an equation $z_2 = f(z_1, \bar{z}_1)$. Far from the

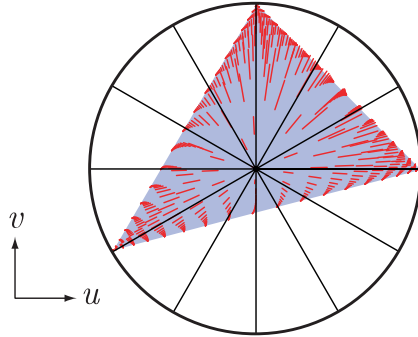


Figure 12: A three-string junction configuration in the MN background projected on the (u, v) -plane.

vertex, each branch of the surface asymptotically approaches a confining string solution, which is represented by

$$y = a_i x + b_i, \quad u = c_i v + d_i, \quad (47)$$

where i is the label of the branch. When we rewrite these relations in terms of complex variables z_1 and z_2 , the function f is holomorphic if the coefficients a_i and c_i are the same. We can always realize $a_i = c_i$ for one i by applying the appropriate rotation of the coordinates u and v . Furthermore, due to the similarity of the triangles displayed in Fig. 2 and Fig. 7, the relation $a_i = c_i$ can be realized for all i simultaneously. Therefore, the function f becomes holomorphic in the asymptotic part of all the branches. We call this property “asymptotic holomorphy”. In terms of real variables, the holomorphy of the function f is represented by the Cauchy-Riemann relations:

$$\left(\frac{\partial v}{\partial u}\right)_x = \left(\frac{\partial y}{\partial x}\right)_u, \quad \left(\frac{\partial y}{\partial u}\right)_x = -\left(\frac{\partial v}{\partial x}\right)_u. \quad (48)$$

In fact, the second equation in (48) is vacuous as a condition for the asymptotic shapes of surfaces. Because we are considering brane configurations which asymptotically approach confining string solutions, the asymptotic forms are always represented by the two factorized equations in (47). Hence, here, the second equation in (48) reduces to the trivial relation $0 = 0$.

This asymptotic holomorphy can be used to check the stability of four-string vertices. Under the assumption of the coincidence of the endpoints of chords, the relation $\theta^f = \theta^v$ for the MN background implies that k chords representing branches of a k -string junction form a k -gon inscribed in the unit circle in the (u, v) -plane. For four-string junctions, there are three cases distinguished by their values of $\theta_{\text{tot}}^f \equiv \sum_{i=1}^4 \theta_i^f$. If $\theta_{\text{tot}}^f = \pi$ or 3π , the squares defined in the (u, v) -plane in this way are similar to the squares composed of the four tension vectors of four external strings, just as in the case of three-string junctions. However, if

$\theta_{\text{tot}}^f = 2\pi$, the inscribed squares are twisted and cannot be similar to the tension squares [see Fig. 13 (a)]. In this case, we obtain squares similar to the tension

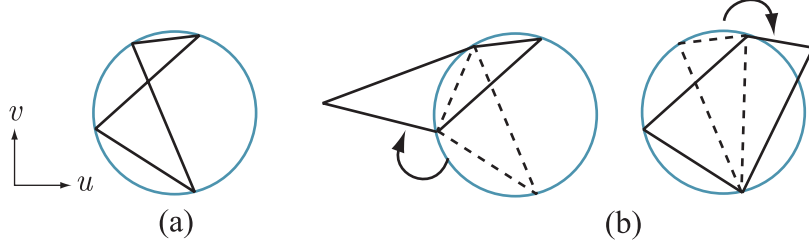


Figure 13: (a) A twisted square for $\theta_{\text{tot}}^f = 2\pi$. (b) Two ways of unfolding.

squares by unfolding the twisted squares. The two ways of unfolding correspond to the two different topologies (H) and (I), which cannot be deformed smoothly into each other [see Fig. 13 (b)]. From these facts, we conclude that a four-string vertex is stable only if it satisfies the asymptotic holomorphy condition, which is equivalent to the similarity of the tension squares and the inscribed squares in the (u, v) -plane.

The asymptotic holomorphy relations are not sufficient to compute the energies of baryon vertices. For this purpose, we need to find some relations that hold everywhere on branes. One possibility is to extend the asymptotic holomorphy to the entire worldvolume as they are. Unfortunately, however, a numerical investigation of generated junction solutions demonstrates that this cannot be done.

In the case of supersymmetric configurations, there is a technique to determine relations holding everywhere on the surface by using Killing spinors. Indeed, various supersymmetric embeddings of D5-branes in the MN background are obtained in Ref. [12] with this technique. Unfortunately, this is not applicable to junction configurations, because they break all the supersymmetries, as mentioned in §3.

The absence of systematic methods compels us to resort to guesswork. Numerically generated junction configurations give important information about how to approach to this problem. Let us consider Fig. 12. The radial pattern of the flux in it implies that $(D^u, D^v) \propto (u, v)$. The proportionality factor can be determined by the Gauss's Law constraint (42), and we obtain the ansatz

$$D'_1 = 2\pi(udv - vdu), \quad D'^a = \frac{2\pi}{\sqrt{\det g_{ab}}} u^a, \quad (49)$$

where $u^a = (u, v)$ and we use the static coordinates $\sigma^a = u^a$. Then, by substituting this ansatz into the energy (45), we obtain

$$E = 2\pi \int d^2\sigma \sqrt{\det \hat{g}_{ab}}, \quad (50)$$

with the effective induced metric \widehat{g}_{ab} defined by

$$\widehat{g}_{ab} = \frac{1}{w}\delta_{ab} + wX_a^i X_b^i, \quad (51)$$

where $X^i = (x, y)$ and $X_a^i = \partial X^i / \partial u^a$. The expression (50) implies that the two-dimensional surfaces can be treated as Nambu-Goto-type branes in the background with the effective metric

$$\widehat{ds}^2 = \frac{1}{w}(du^2 + dv^2) + w(dx^2 + dy^2). \quad (52)$$

Thus, it is quite natural to replace du , dv , dx , and dy in the Cauchy-Riemann relations (48) by $w^{-1/2}du$, $w^{-1/2}dv$, $w^{1/2}dx$, and $w^{1/2}dy$, respectively. As a result, we obtain the following “modified Cauchy-Riemann relations”, which take the place of the holomorphy for (p, q) -string junctions:

$$\left(\frac{\partial v}{\partial u}\right)_x = \left(\frac{\partial y}{\partial x}\right)_u, \quad w \left(\frac{\partial y}{\partial u}\right)_x = -\frac{1}{w} \left(\frac{\partial v}{\partial x}\right)_u. \quad (53)$$

Note that these relations do not contradict the asymptotic holomorphy relations (48) but, rather, guarantee them. Because the relation between (x, u) and (y, v) is factorized as (47) in asymptotic regions, the second relation in (53) becomes trivial as the second relation in (48).

We can show that the equations of motion are automatically satisfied if the shape of a brane satisfies the modified Cauchy-Riemann relations (53) and the flux density on it is given by the ansatz (49). The equation of motion for X^i obtained from the energy (50) is

$$\partial_a \left(\sqrt{\det \widehat{g}_{ab} w} \widehat{g}^{ab} X_b^i \right) = 0. \quad (54)$$

In order to obtain the equation of motion for the gauge field, we should use the action (45), to which the ansatz (49) has not been applied. With variations in the form $\delta D^a = (1/\sqrt{g})\epsilon^{ab}\partial_b\phi$, which do not violate the constraint (42), we obtain the Maxwell’s equation for the electric field strength E_a ,

$$\epsilon^{ab}\partial_a E_b = 0, \quad (55)$$

where the relation between E_a and D^a is

$$E_a = \frac{g_{ab}D^a}{\sqrt{(2\pi w)^2 + g_{ab}D^a D^b}}. \quad (56)$$

This can be rewritten using the ansatz (49) as

$$E_a = \frac{g_{ab}u^b}{\sqrt{\det \widehat{g}_{ab}}} = \frac{\widehat{g}_{ab}u^b}{w\sqrt{\det \widehat{g}_{ab}}}. \quad (57)$$

To show that equations of motion (54) and (55) hold, we first rewrite the relations (53) in terms of the functions $x(u, v)$ and $y(u, v)$. Then, using the chain rule for partial derivatives, we obtain

$$x_u + y_v = 0, \quad x_u y_v - y_u x_v = \frac{1}{w^2}, \quad (58)$$

or equivalently,

$$\text{tr } X_a^i = 0, \quad \det X_a^i = \frac{1}{w^2}. \quad (59)$$

(Here and hereafter, when subscripts are used to represent derivatives, the independent variables are always u and v .) Using these relations, the effective metric (51) becomes

$$\hat{g}_{ab} = w(X_a^i X_b^i + \delta_{ab} \det X_a^i) = w(x_v - y_u) \begin{pmatrix} -y_u & -y_v \\ x_u & x_v \end{pmatrix}, \quad (60)$$

and its determinant is

$$\det \hat{g}_{ab} = (x_v - y_u)^2. \quad (61)$$

With the help of (60) and (61), we can easily show that the equations of motion (54) and (55) are indeed satisfied.

Although we have shown that the modified Cauchy-Riemann relations (53) and the ansatz (49) guarantee that brane configurations satisfy the equations of motion (54) and (55), the converse is not true, as there exist solutions of equations of motion which do not satisfy the modified Cauchy-Riemann relations and the D -field ansatz. An example of such a configuration is the deformed baryon configuration given in Ref. [56]. Such configurations, however, do not approach confining string solutions asymptotically, and their existence does not invalidate the arguments given in this section.

Now, we are ready to prove the vanishing of the energies of baryon vertices analytically. From (50) and (61), the energy $E_{\text{junc}}(L)$ defined above (46) is given by

$$E_{\text{junc}}(L) = 2\pi \int_J dudv |x_v - y_u| = 2\pi \left| \oint_{\partial J} (xdu + ydv) \right|, \quad (62)$$

where J is the region in a junction worldvolume determined by the relation $x^2 + y^2 \leq L^2$. Before applying Stokes' theorem to (62), the absolute value should be moved out of the integral. This is possible, because as shown by (58), $x_v - y_u$ never vanishes on the worldvolume. The boundary ∂J consists of two kinds of boundaries, which we call A-boundaries (the solid lines in Fig. 14) and B-boundaries (the dashed lines in Fig. 14). The A-boundaries are the edges of the surface on the boundary $u^2 + v^2 = 1$ of the target space. The B-boundaries arise due to the cut off $x^2 + y^2 = L$. The A-boundaries are mapped to apices of the triangle when they are projected on the (u, v) -plane, and the coordinates u and v are constants on them. Therefore, the A-boundaries do not contribute

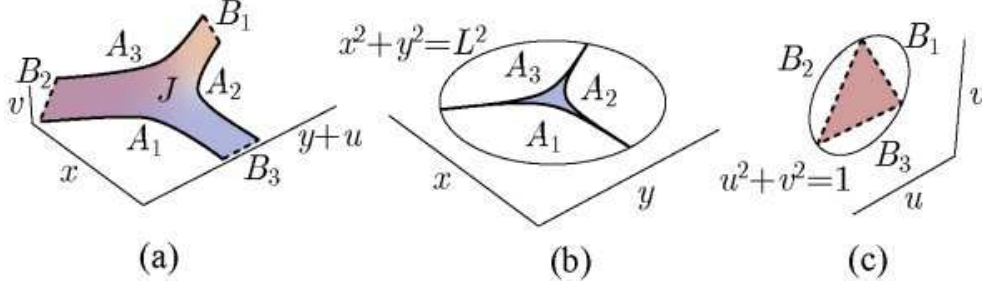


Figure 14: (a) J and its boundary. (b) The projection on the (x, y) -plane. (c) The projection on the (u, v) -plane.

to the contour integral in (62). Thus, we need only consider the integral on the B-boundaries. If L is sufficiently large, each B-boundary is mapped to a point by the projection in the (x, y) -plane. Let (x_i, y_i) be the point corresponding to the i -th B-boundary, B_i . These are on the circle $x^2 + y^2 = L^2$, and we can write

$$(x_i, y_i) = L(\alpha_i, \beta_i), \quad (\alpha_i^2 + \beta_i^2 = 1) \quad (63)$$

where (α_i, β_i) is a unit vector representing the direction of the i -th branch in the (x, y) -plane. If we project the B-boundaries to the (u, v) -plane, they are mapped to sides of the triangle when L is sufficiently large. Due to the similarity between this triangle and the tension triangle, which is guaranteed by the modified Cauchy-Riemann relations (53), the integration measure (du_i, dv_i) on B_i can be represented as

$$(du_i, dv_i) = \pm(\alpha_i, \beta_i)dl_i, \quad (64)$$

where the signature depends on the orientation of the contour, and dl_i is an infinitesimal length on the i -th side of the triangle in the (u, v) -plane. Combining (63) and (64), we obtain the following expression for the energy of a junction:

$$E_{\text{junc}} = 2\pi \sum_i L \int_{B_i} dl_i = 2\pi \sum_i L \times 2 \sin \theta_i^f = \sum_i LT(\theta_i^f). \quad (65)$$

Here, we have used the fact that the integral $\int_{B_i} dl_i$ gives the length of the i -th side of the triangle $2 \sin \theta_i^f$ and the tension formula (31) for the MN background. The result (65) implies that the energy of a junction is given by the sum of the energies of the branches and that there is no vertex contribution.

Now we can answer the question raised at the end of §2. Although the expression (21) seemingly depends on g_{str} , which has no counterpart in the boundary field theory of the MN solution, $\tilde{E}_{\text{vertex}}$ on the right-hand side is actually zero, and the energies of the baryon vertices in fact are independent of g_{str} .

7 Conclusions

In this paper, we have investigated string junctions in $\mathcal{N} = 1$ supersymmetric gauge theories in the context of the gauge/gravity correspondence. We have used the Maldacena-Núñez and the Klebanov-Strassler solutions as gravity duals of the confining gauge theories.

In §3 we studied the balance of the tensions for three-string junctions and planar four-string junctions. We found that four-string vertices are stable only in the case that $\theta_{\text{tot}}^f = \pi$ or 3π in the MN solution. Planar four-string vertices in the KS solution are always unstable. It may be interesting to generalize this consideration to non-planar junctions.

In §5, we reported the results of numerical computations of the energies of baryon vertices, and we found that in the KS case the energies are negative, while in the MN case they almost vanish. The vanishing of the energies strongly suggests that the brane configurations in the MN background possess some analytic structure which guarantees this vanishing. Indeed, we discovered relations similar to the Cauchy-Riemann relations for holomorphic surfaces. With the help of these relations, we analytically proved the disappearance of the energies of baryon vertices.

We should emphasize that the analysis given in this paper is classical. As mentioned in §3, the existence of confining strings breaks all the supersymmetries. Thus, there is no mechanism to control quantum corrections, and our results are justified only in the limit of large N and large Ng_{str} , in which the background curvature is small compared to the string scale and the Plank scale.

In order to investigate realistic baryons in non-supersymmetric QCD, we have to use different gravity backgrounds. For example, we can use an AdS Schwarzschild black hole[4, 57]. Because the IR geometry of this solution has structure similar to the KS and MN solutions, we can study junction configurations in it in a manner similar to that used in this paper.

We have treated only brane configurations embedded in the IR geometry in this paper. They can be used for highly-excited baryons, in which the endpoints of strings are separated from each other. To analyze ground-state baryons, we should consider different kinds of brane configurations that consist of a baryon vertex and only one external string going up along the r direction to flavor branes. The external string in this case represents coincident quarks. It is important to determine whether such branes are stable, and if so, to investigate their energies and excitations.

There are many interesting problems associated with brane constructions of hadrons in addition to those mentioned above. We hope to return to these issues in the near future.

Acknowledgements

I would like to thank M. Bando and A. Sugamoto for motivating me to do this work. I also thank F. Koyama, H. Ooguri, S. Sugimoto and M. Tachibana for valuable discussions. This work is supported in part by a Grant-in-Aid for the Encouragement of Young Scientists (#15740140) from the Japan Ministry of Education, Culture, Sports, Science and Technology, and by the Rikkyo University Special Fund for Research.

A

A.1 Treatment of flux on triangulated surfaces

The purpose of this section is to explain how to discretize branes with flux flowing on them and how to vary variables while maintaining the Gauss's Law constraint.

To compute the energy of a D3-brane, which is represented in (45) as an integral over a two-dimensional surface, we first triangulate the surface. We label sites by i, j, k, \dots and each oriented link by two labels representing its two ends. The functions $X^I(\sigma^a)$ describing the shape of the surface are replaced by the variables $X_i^I = (x_i, y_i, u_i, v_i, w_i)$ on the sites, with the constraints $u_i^2 + v_i^2 + w_i^2 = 1$ and $w_i \geq 0$. To represent the flux density, we use link variables

$$\phi_{ij} \equiv \int_i^j D_1^I, \quad (66)$$

where the integral is carried out along the link ij . This represents the amount of flux flowing across the link ij . We define the orientation in such a way that if the arrow from site i to j is upward, ϕ_{ij} represents the flux passing the link ij from left to right. By definition we have

$$\phi_{ij} = -\phi_{ji}. \quad (67)$$

The area of a triangle ijk is denoted by s_{ijk} (see Fig. 15). This area is a real

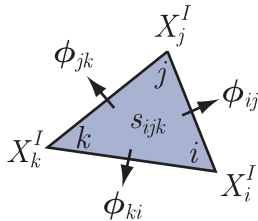


Figure 15: The triangle ijk . X_i^I denotes the coordinate of the vertex i . ϕ_{ij} represents the flux flowing across the link ij . The area of the triangle ijk is denoted by s_{ijk} .

positive number. We also define s'_{ijk} as the area of the triangle ijk projected on the (u, v) -plane. This take either a positive or negative value, depending on the orientation of the triangle. s_{ijk} and s'_{ijk} are easily represented as functions of the variables X_i^I , X_j^I and X_k^I .

Given the variables X_i^I and ϕ_{ij} , the energy of the D3-brane is obtained as the discretized version of the energy (45),

$$E = \sum_{\text{triangles}} s_{ijk} \sqrt{(2\pi w_{ijk})^2 + \sum_I (D_{ijk}^I)^2}, \quad (68)$$

where w_{ijk} is the w -component of the center of mass $X_{ijk}^I = (X_i^I + X_j^I + X_k^I)/3$ of the triangle ijk , and D_{ijk}^I is the push-forward of the electric flux density to the five-dimensional space (x, y, u, v, w) , which is given by

$$D_{ijk}^I = \frac{1}{2s_{ijk}} \{ \phi_{jk}(X_i^I - X_{ijk}^I) + \phi_{ki}(X_j^I - X_{ijk}^I) + \phi_{ij}(X_k^I - X_{ijk}^I) \}. \quad (69)$$

A discretized version of the Gauss's Law constraint is

$$\phi_{ij} + \phi_{jk} + \phi_{ki} = 2\pi\rho s'_{ijk}. \quad (70)$$

In order to find a configuration that minimizes the energy, we should vary the variables X_i^I and ϕ_{ij} in such manner that does not violate this Gauss's Law constraint.

There are two kinds of variations. Variations of ϕ_{ij} with fixed X_i^I are generated by the following variation for each site i :

$$\phi_{ji} \rightarrow \phi_{ji} + c, \quad j \in \text{Adj}(i). \quad (71)$$

Here, $\text{Adj}(i)$ represents the set of all the sites adjoining the site i . This variation changes the rotation of the flux density around the site i [see Fig. 16 (a)]. The other kind of variations are those that change X_i^I . Even when we vary the variables X_i^I , we should take account of the Gauss's Law constraint (70), because variations of X_i^I change charges in triangles. If the position of a site i moves from X_i^I to $X_{i'}^I = X_i^I + \delta X_i^I$, the projected area s'_{ijk} of the triangle ijk is changed by the amount $s'_{jii'} - s'_{kii'}$ [see Fig. 16 (b)]. To maintain the Gauss's Law constraint (70), we must change the flux variables simultaneously according to the relation

$$\phi_{ki'} = \phi_{ki} - 2\pi\rho s'_{kii'}, \quad k \in \text{Adj}(i). \quad (72)$$

Any continuous deformation can be generated by the two kinds of variations (71) and (72).

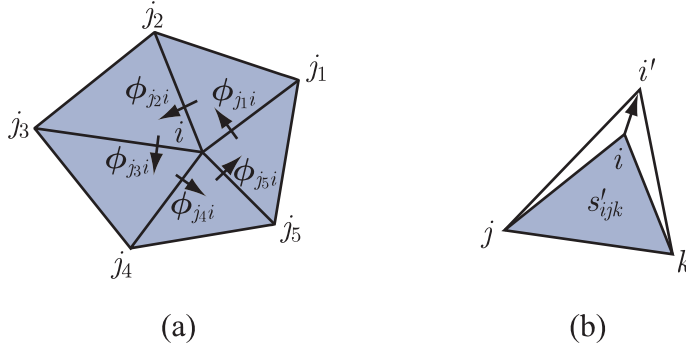


Figure 16: (a) A variation changing the rotation of the electric flux density around i while maintaining the Gauss's Law constraint. (b) If a site i moves to i' , the projected areas of the triangles that possesses this site as a corner change.

References

- [1] J. M. Maldacena, “*The Large N Limit of Superconformal Field Theories and Supergravity*”, *Adv.Theor.Math.Phys.* **2** (1998) 231-252; *Int.J.Theor.Phys.* **38** (1999) 1113-1133, [hep-th/9711200](#).
- [2] S. S. Gubser, I. R. Klebanov, A. M. Polyakov, “*Gauge Theory Correlators from Non-Critical String Theory*”, *Phys.Lett.* **B428** (1998) 105-114, [hep-th/9802109](#).
- [3] E. Witten, “*Anti De Sitter Space And Holography*”, *Adv.Theor.Math.Phys.* **2** (1998) 253-291, [hep-th/9802150](#).
- [4] E. Witten, “*Anti-de Sitter Space, Thermal Phase Transition, And Confinement In Gauge Theories*”, *Adv.Theor.Math.Phys.***2** (1998) 505-532, [hep-th/9803131](#).
- [5] D. J. Gross, H. Ooguri, “*Aspects of Large N Gauge Theory Dynamics as Seen by String Theory*”, *Phys.Rev.* **D58** (1998) 106002, [hep-th/9805129](#).
- [6] C. Csaki, H. Ooguri, Y. Oz, J. Terning, “*Glueball Mass Spectrum From Supergravity*”, *JHEP* **9901** (1999) 017, [hep-th/9806021](#).
- [7] H. Ooguri, H. Robins, J. Tannenhauser, “*Glueballs and Their Kaluza-Klein Cousins*”, *Phys.Lett.* **B437** (1998) 77-81, [hep-th/9806171](#).
- [8] A. Karch, E. Katz, N. Weiner, “*Hadron Masses and Screening from AdS Wilson Loops*”, *Phys.Rev.Lett.* **90** (2003) 091601, [hep-th/0211107](#).
- [9] M. Kruczenski, D. Mateos, R. C. Myers, D. J. Winters, “*Meson Spectroscopy in AdS/CFT with Flavour*”, *JHEP* **0307** (2003) 049, [hep-th/0304032](#).

- [10] T. Sakai, J. Sonnenschein, “*Probing Flavored Mesons of Confining Gauge Theories by Supergravity*”, JHEP **0309** (2003) 047, hep-th/0305049.
- [11] J. Babington, J. Erdmenger, N. Evans, Z. Guralnik, I. Kirsch, “*Chiral Symmetry Breaking and Pions in Non-Supersymmetric Gauge/Gravity Duals*”, Phys.Rev. **D69** (2004) 066007, hep-th/0306018.
- [12] C. Nunez, A. Paredes, A. V. Ramallo, “*Flavoring the Gravity Dual of $N=1$ Yang-Mills with Probes*”, JHEP **0312**(2003)024, hep-th/0311201
- [13] E. Schreiber, “*Excited Mesons and Quantization of String Endpoints*”, hep-th/0403226.
- [14] S. Hong, S. Yoon, M. J. Strassler, “*On the Couplings of Vector Mesons in AdS/QCD*”, hep-th/0409118.
- [15] M. Kruczenski, L. A. P. Zayas, J. Sonnenschein, D. Vaman “*Regge Trajectories for Mesons in the Holographic Dual of Large- N_c QCD*”, hep-th/0410035.
- [16] E. Witten, “*Baryons And Branes In Anti de Sitter Space*”, JHEP **9807** (1998) 006, hep-th/9805112.
- [17] A. Brandhuber, N. Itzhaki, J. Sonnenschein, S. Yankielowicz, “*Baryons from Supergravity*”, JHEP **9807** (1998) 020, hep-th/9806158.
- [18] Y. Imamura, “*Supersymmetries and BPS Configurations on Anti-de Sitter Space*”, Nucl.Phys. **B537** (1999) 184-202, hep-th/9807179.
- [19] C. G. Callan, A. Guijosa, K. G. Savvidy, “*Baryons and String Creation from the Fivebrane Worldvolume Action*”, Nucl.Phys. **B547** (1999) 127-142, hep-th/9810092.
- [20] D. Berenstein, C. P. Herzog, I. R. Klebanov, “*Baryon Spectra and AdS/CFT Correspondence*”, JHEP **0206** (2002) 047, hep-th/0202150.
- [21] J. Polchinski, M. J. Strassler, “*Hard Scattering and Gauge/String Duality*”, Phys.Rev.Lett. **88** (2002) 031601, hep-th/0109174.
- [22] J. Polchinski, M. J. Strassler, “*Deep Inelastic Scattering and Gauge/String Duality*”, JHEP **0305** (2003) 012, hep-th/0209211.
- [23] E. G. Gimon, L. A. P. Zayas, J. Sonnenschein, M. J. Strassler, “*A Soluble String Theory of Hadrons*”, JHEP **0305** (2003) 039, hep-th/0212061.
- [24] R. Apreda, F. Bigazzi, A. L. Cotrone “*Strings on pp-waves and Hadrons in (softly broken) $N=1$ gauge theories*”, JHEP **0312** (2003) 042, hep-th/0307055.

- [25] S. Kuperstein, J. Sonnenschein, “*Analytic non-supersymmetric background dual of a confining gauge theory and the corresponding plane wave theory of Hadrons*”, JHEP **0402** (2004) 015, hep-th/0309011.
- [26] M. Schvellinger, “*Spinning and rotating strings for $N=1$ SYM theory and brane constructions*”, JHEP **0402** (2004) 066, hep-th/0309161.
- [27] G. Bertoldi, F. Bigazzi, A. L. Cotrone, C. Núñez, L. A. P. Zayas, “*On the Universality Class of Certain String Theory Hadrons*”, hep-th/0401031.
- [28] F. Bigazzi, A. L. Cotrone, L. Martucci, “*Semiclassical spinning strings and confining gauge theories*”, Nucl.Phys. **B694** (2004) 3-34, hep-th/0403261.
- [29] F. Bigazzi, A. L. Cotrone, L. Martucci, L. A. P. Zayas, “*Wilson Loop, Regge Trajectory and Hadron Masses in a Yang-Mills Theory from Semiclassical Strings*”, hep-th/0409205.
- [30] M. Bando, T. Kugo, A. Sugamoto, S. Terunuma, “*Pentaquark Baryons in String Theory*”, Prog.Theor.Phys. **112** (2004) 325-355, hep-ph/0405259.
- [31] T. Nakano et al. (LEPS collaboration), Phys. Rev. Lett. **91** (2003), 012000.
- [32] C. Alt et al. (NA49 collaboration), hep-ex/0310014.
- [33] A. Karch, E. Katz, “*Adding flavor to AdS/CFT*”, JHEP **0206** (2002) 043, hep-th/0205236.
- [34] S. -J. Rey, J. -T. Yee, “*Macroscopic strings as heavy quarks: Large- N gauge theory and anti-de Sitter supergravity*”, Eur.Phys.J. **C22** (2001) 379-394, hep-th/9803001.
- [35] J. M. Maldacena, “*Wilson loops in large N field theories*”, Phys.Rev.Lett.**80** (1998) 4859-4862, hep-th/9803002.
- [36] C. P. Herzog, I. R. Klebanov, “*On String Tensions in Supersymmetric $SU(M)$ Gauge Theory*”, Phys.Lett. **B526** (2002) 388-392, hep-th/0111078.
- [37] R. C. Myers, “*Dielectric-Branes*”, JHEP **9912** (1999) 022, hep-th/9910053.
- [38] J. Maldacena, C. Núñez, “*Supergravity description of field theories on curved manifolds and a no go theorem*”, Int.J.Mod.Phys. **A16** (2001) 822-855, hep-th/0007018.
- [39] J. M. Maldacena, C. Núñez, “*Towards the large N limit of pure $N=1$ super Yang Mills*”, Phys.Rev.Lett. **86** (2001) 588-591, hep-th/0008001.
- [40] I. R. Klebanov, N. A. Nekrasov, “*Gravity Duals of Fractional Branes and Logarithmic RG Flow*”, Nucl.Phys. **B574** (2000) 263-274, hep-th/9911096.

- [41] I. R. Klebanov, M. J. Strassler, “*Supergravity and a Confining Gauge Theory: Duality Cascades and χ SB-Resolution of Naked Singularities*”, JHEP **0008** (2000) 052, hep-th/0007191.
- [42] C. P. Herzog, I. R. Klebanov, P. Ouyang, “*D-Branes on the Conifold and $N=1$ Gauge/Gravity Dualities*”, hep-th/0205100.
- [43] X. -J. Wang, S. Hu, “*Intersecting branes and adding flavors to the Maldacena-Nunez background*”, JHEP **0309** (2003) 017, hep-th/0307218.
- [44] S. S. Gubser, I. R. Klebanov “*Baryons and Domain Walls in an $N = 1$ Superconformal Gauge Theory*”, Phys.Rev. **D58** (1998) 125025, hep-th/9808075.
- [45] I.R. Klebanov, A.A. Tseytlin, “*Gravity Duals of Supersymmetric $SU(N) \times SU(N+M)$ Gauge Theories*”, Nucl.Phys. **B578** (2000) 123-138, hep-th/0002159.
- [46] S. S. Gubser, C. P. Herzog, I. R. Klebanov, “*Symmetry Breaking and Axionic Strings in the Warped Deformed Conifold*”, hep-th/0405282.
- [47] M. Schvellinger, “*Glueballs, symmetry breaking and axionic strings in non-supersymmetric deformations of the Klebanov-Strassler background*”, JHEP **0409** (2004) 057, hep-th/0407152.
- [48] E. Witten, “*Noncommutative Geometry And String Field Theory*”, Nucl.Phys. **B268** (1986) 253.
- [49] J. H. Schwarz, “*Lectures on Superstring and M Theory Dualities*”, Nucl.Phys.Proc.Suppl. **55B** (1997) 1-32, hep-th/9607201.
- [50] O. Aharony, J. Sonnenschein, S. Yankielowicz, “*Interactions of strings and D-branes from M theory*”, Nucl.Phys. **B474** (1996) 309-322, hep-th/9603009.
- [51] K. Dasgupta, S. Mukhi, “*BPS Nature of 3-String Junctions*”, Phys.Lett. **B423** (1998) 261-264, hep-th/9711094.
- [52] A. Sen, “*String Network*”, JHEP **9803** (1998) 005, hep-th/9711130.
- [53] S. -J. Rey, J. -T. Yee, “*BPS Dynamics of Triple (p,q) String Junction*”, Nucl.Phys. **B526** (1998) 229-240, hep-th/9711202.
- [54] M. Krogh, S. Lee, “*String Network from M-theory*”, Nucl.Phys. **B516** (1998) 241-254, hep-th/9712050.
- [55] Y. Matsuo, K. Okuyama, “*BPS Condition of String Junction from M theory*”, Phys.Lett. **B426** (1998) 294-296, hep-th/9712070.

- [56] S. A. Hartnoll, R. Portugues, “*Deforming baryons into confining strings*”, hep-th/0405214.
- [57] S. W. Hawking, D. Page, “*Thermodynamics Of Black Holes In Anti-de Sitter Space*”, Commun. Math. Phys. **87** (1983) 577.